[6] E. G. Crystal and S. Frankel, "Design of hairpin-line and hybrid hairpin-line-parallel-coupled-line filters," *IEEE G-MTT Symp. Dig.*, pp. 12–13, 1971.
[7] T. G. Bryant and J. A. Weiss, "Parameters of microstrip transmission lines and of coupled pairs of microstrip lines," *IEEE Trans. Microwave Theory Tech. (1968 Symp. Issue)*, vol. MTT-16 pp. 1021–1027, Dec. 1968.
[8] M. A. R. Gunston, *Microwave Transmission Line Impedance Data*. London: Van Nostrand Reinhold, 1972.
[9] M. K. Krage and G. I. Haddad, "Frequency-dependent characteristics of microstrip transmission lines," *IEEE Trans. Microwave Theory Tech.*, vol. MTT-20, pp. 678–688, Oct. 1972.
[10] R. Horton, "Loss calculations of coupled microstrip lines," *IEEE Trans. Microwave Theory Tech.* (Short Papers), vol. MTT-21, pp. 359–360, May 1973.

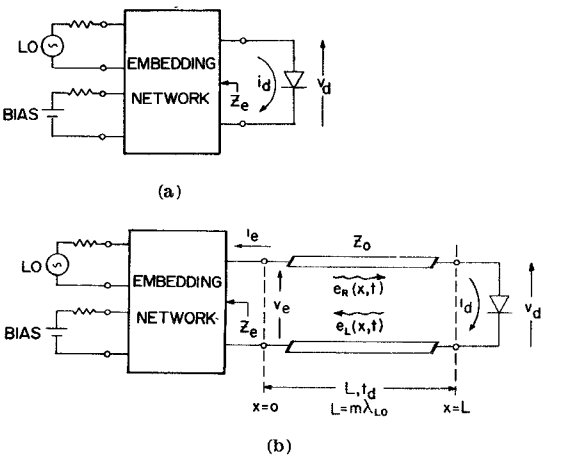

Fig. 1. (a) The mixer circuit for which v_d and i_d are to be determined. (b) The modified circuit which has the same steady-state v_d and i_d provided L is an integral number of wavelengths at the LO frequency. The right- and left-propagating waves on the transmission line are denoted by e_R and e_L.

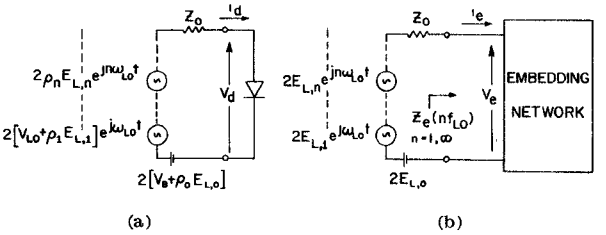

Fig. 2. The two circuits whose steady-state solutions are alternately computed to determine the steady-state solution of Fig. 1(b). The simple nonlinear circuit (a) is solved in the time domain, the linear circuit (b) in the frequency domain. Source amplitudes are given by (9)–(11).

A Technique for Determining the Local Oscillator Waveforms in a Microwave Mixer

A. R. KERR, ASSOCIATE MEMBER, IEEE

***Abstract*—A technique is described which enables the large-signal current and voltage waveforms to be determined for a mixer diode. This technique is applicable to any configuration where the impedance seen by the diode at the local oscillator (LO) frequency and its harmonics is known.**

I. INTRODUCTION

The performance of a diode mixer is largely determined by the current and voltage waveforms produced at the diode by the local oscillator (LO). These waveforms depend on the diode itself, and on the impedance of its embedding network at the LO frequency and its harmonics. This short paper describes a method for computing the diode current and voltage waveforms for any mixer in which the impedance seen by the diode at the LO frequency and its harmonics is known.

In the past there have been various approaches to this problem. Torrey and Whitmer [1] and others have assumed a sinusoidal driving voltage at the diode, all the harmonics of the LO being assumed to be short-circuited. Fleri and Cohen [2] used both digital and analog computers to solve the nonlinear problem, assuming simple lumped-element embedding networks.

Egami [3] and Gwarek [4] have used a harmonic balance approach in the frequency domain. However, convergence has been found difficult to achieve for some circuits when many harmonics are considered, and especially at large LO drive levels; and the initial guess has a strong effect on the rate of convergence.

A recent approach by Gwarek [4] uses a time-domain analysis to determine the diode waveforms in an embedding network consisting of a simple lumped-element network in series with a string of voltage sources, one at each harmonic of the LO. The voltage sources are input-voltage dependent so that the embedding network is able to simulate any complex network as it appears at the LO frequency and its harmonics. It is reported that this method is convergent, and more economical of computer time and memory than the harmonic balance technique.

In the approach described here, the circuit of Fig. 1(a) is modified by the insertion of a transmission line, Fig. 1(b), which, by virtue of its electrical length at the LO frequency and its harmonics, has no effect on the steady-state solution of the problem. It will be shown that this enables the problem to be solved iteratively by alternately solving the simpler circuit problems shown in Fig. 2(a) and (b).

Hypothesis: The steady-state i_d and v_d waveforms for the two circuits of Fig. 1 are the same. Certainly the solution for Fig. 1(b) is a valid solution for Fig. 1(a), but there exists the possibility of more than one steady-state solution for Fig. 1(a), the one which is finally reached being determined by the particular path taken to reach the steady state.[1] An hypothesis equivalent to this one is implicit in any method of solution in which the calculation of the actual turn-on transient is bypassed.

II. METHOD

Consider the circuit of Fig. 1(b) with the diode initially disconnected. When the diode is connected transient reflections occur alternately at the two ends of the transmission line until eventually the steady-state condition is approached. In the steady state, waves of constant amplitude, containing many LO harmonics generated by the diode, propagate in each direction. The approach taken here is to let the transmission line become so long that in the periods between transient reflections a steady-state condition is reached

Manuscript received October 4, 1974; revised May 2, 1975. This work was supported by Associated Universities, Inc., under contract with the National Science Foundation.

The author was with the National Radio Astronomy Observatory, Charlottesville, Va. 22901. He is now with the NASA Goddard Institute for Space Studies, New York, N. Y. 10025.

[1] As an example of this, it has been observed that for some mixers, as the LO power is increased from zero, parametric oscillation will occur. At higher power levels the oscillation ceases, and it cannot be made to reappear unless the LO power is first reduced below some threshold value and then increased again.

between the transmission line and the diode on the one hand, and between the transmission line and the embedding network on the other. The problem then reduces to that of alternately determining the steady-state solutions for the two simple circuits of Fig. 2, each time changing the voltage sources in a predetermined way, until the terminal currents and voltages are the same for the two circuits.

For clarity, a simple exponential diode will be assumed in describing the method: the inclusion of diode capacitance and series resistance will be described later. For the simple diode

$$i_d = i_0[\exp(\alpha v_d) - 1]. \tag{1}$$

The right- and left-propagating waves on the transmission line are denoted by $e_R(x,t)$ and $e_L(x,t)$ as shown in Fig. 1(b). These waves must conform to the boundary condition imposed by (1), with

$$e_R(L,t) + e_L(L,t) = v_d(t) \tag{2a}$$

and

$$[e_R(L,t) - e_L(L,t)]/Z_0 = i_d(t). \tag{2b}$$

At the left-hand end of the transmission line the voltage and current are

$$v_e(t) = e_L(0,t) + e_R(0,t) \tag{3a}$$

and

$$i_e(t) = [e_L(0,t) - e_R(0,t)]/Z_0. \tag{3b}$$

It is convenient to express v_e and i_e as Fourier series

$$v_e(t) = \sum_{n=0}^{\infty} V_{e,n} \exp(jn\omega_{LO}t) \tag{4a}$$

and

$$i_e(t) = \sum_{n=0}^{\infty} I_{e,n} \exp(jn\omega_{LO}t) \tag{4b}$$

where the Fourier coefficients $V_{e,n}$ and $I_{e,n}$ are, in general, complex. The steady-state boundary condition defined by the embedding network is

$$\frac{V_{e,n}}{I_{e,n}} = Z_e(jn\omega_{LO}), \qquad n > 1 \tag{5a}$$

$$\frac{V_{e,1} - V_{LO}}{I_{e,1}} = Z_e(j\omega_{LO}) \tag{5b}$$

and

$$\frac{V_{e,0} - V_B}{I_{e,0}} = Z_e(0) \tag{5c}$$

where V_{LO} and V_B are the open-circuit LO and dc voltages of the embedding network.

The solution is commenced at time $t = 0$ when the diode is first connected to the circuit of Fig. 1(b). The equivalent circuit of Fig. 2(a) applies, but with only two voltage sources, V_B at dc, and V_{LO} at the LO frequency. For the simple diode assumed in this example $v_d(t)$ and $i_d(t)$ are easily computed. During the time interval $0 < t < 2t_d$

$$e_R(L,t) = V_B + V_{LO} \exp(j\omega_{LO}t) \tag{6a}$$

and

$$e_L(L,t) = v_d(t) - i_d(t)Z_0 \tag{6b}$$

where t_d is the propagation delay on the transmission line. At the left-hand end of the transmission line the left-propagating wave is

$$e_L(0,t) = e_L(L,t - t_d). \tag{7}$$

Since e_L is composed only of the LO frequency and its harmonics for which the transmission line is an integral number of wavelengths long

$$e_L(L,t - t_d) = e_L(L,t). \tag{8}$$

Therefore, during the time interval $t_d < t < 3t_d$

$$e_L(0,t) = v_d(t) - i_d(t)Z_0. \tag{9}$$

Expressing (9) as a Fourier series gives

$$e_L(0,t) = \sum_{n=0}^{\infty} E_{L,n} \exp(jn\omega_{LO}t). \tag{10}$$

The embedding network reaches steady state after some time δ so that in the interval $t_d + \delta < t < 3t_d$ a new steady-state right-propagating wave $e_R(0,t)$ exists. This may be determined knowing the complex reflection coefficient of the embedding network at each harmonic of the LO

$$\rho_n = \frac{Z_e(jn\omega_{LO}) - Z_0}{Z_e(jn\omega_{LO}) + Z_0}. \tag{11}$$

Then

$$e_R(0,t) = V_B + V_{LO} \exp(j\omega_{LO}t) + \sum_{n=0}^{\infty} \rho_n E_{L,n} \exp(jn\omega_{LO}t). \tag{12}$$

Again e_R contains only components at the LO frequency and its harmonics, and so after the appropriate delay time t_d we have

$$e_R(L,t) = e_R(0,t). \tag{13}$$

This applies during the time interval $2t_d + \delta < t < 4t_d$. The diode voltage and current $v_d(t)$ and $i_d(t)$ are again calculated, giving the next value of $e_L(L,t)$ from (6b), which commences the next cycle of iteration.

Summary of Iteration Cycle

The typical cycle of iteration may be summarized as follows.

Step 1): From the diode voltage and current, $v_d(t)$ and $i_d(t)$, compute the left-propagating wave $e_L(L,t)$ using (6b).

Step 2): After a time t_d the left-propagating wave reaches the embedding network causing a response which reaches steady state after a further time δ. Since the transmission line can be made as long as required, it is always possible to ensure that $\delta \ll t_d$. The new steady-state right-propagating wave at the embedding network $e_R(0,t)$ is calculated using (11) and (12).

Step 3): After a further propagation delay t_d this wave becomes the new right-propagating wave at the diode, $e_R(L,t)$ from which new values of diode voltage and current are computed using the equivalent circuit of Fig. 2(a).

Convergence

Under steady-state operation the voltages and currents at the two ends of the transmission line are equal—that is $v_d(t) = v_e(t)$ and $i_d(t) = -i_e(t)$. In the frequency domain this is equivalent to

$$V_{d,n} = V_{e,n} \tag{14a}$$

and

$$I_{d,n} = -I_{e,n} \tag{14b}$$

where $V_{d,n}$, $I_{d,n}$, $V_{e,n}$, and $I_{e,n}$ are the nth Fourier coefficients of v_d, i_d, v_e, and i_e, respectively. It follows that

$$\frac{V_{d,n}}{I_{d,n}} = -\frac{V_{e,n}}{I_{e,n}}. \tag{15}$$

It is convenient to define a *diode impedance*

$$Z_d(jn\omega_{LO}) = V_{d,n}/I_{d,n}. \tag{16}$$

Then with (5a) and (15)

$$Z_d(jn\omega_{LO}) = -Z_e(jn\omega_{LO}), \qquad \text{for} \quad n > 1. \tag{17}$$

We define a convergence parameter

$$|Z_d(jn\omega_{LO})|/|Z_e(jn\omega_{LO})|, \qquad n > 1$$

which must be equal to unity for a completely converged solution. For the example given in the following (Fig. 3), the convergence parameter is shown in Fig. 4 as a function of n.

The choice of the hypothetical transmission-line characteristic impedance Z_0 has some effect on the rate of convergence of the solution. A value of 50 Ω has been used in the example; the effects of varying it have not been investigated in detail.

Finite Number of Harmonics

In a practical computer solution of the mixer problem it is possible to consider only a finite number N of harmonics of the LO. This is electrically equivalent to defining the embedding impedance for the higher LO harmonics equal to the transmission-line characteristic impedance

$$Z_e(jn\omega_{LO}) = Z_0, \qquad n > N. \tag{18}$$

To show this equivalence, consider the circuit of Fig. 1(b), with Z_e as defined in (18), so that $\rho_n = 0$ for $n > N$ (11). From (12) and (13) we see that the right-propagating wave $e_R(L,t)$ contains no frequency components above the Nth LO harmonic. It follows that there are no voltage sources above the Nth harmonic in the circuit of Fig. 2(a), and that the computed v_d and i_d waveforms are the same (up to the Nth harmonic) as would be computed for the mixer if (18) were not valid and if all harmonics above the Nth were neglected in the computation.

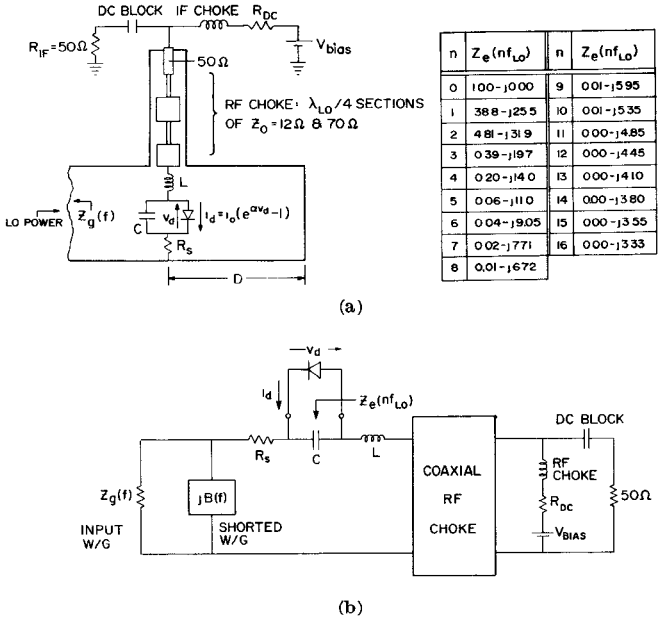

n	$Z_e(nf_{LO})$	n	$Z_e(nf_{LO})$
0	100-j000	9	001-j595
1	388-j255	10	001-j535
2	481-j319	11	000-j485
3	039-j197	12	000-j445
4	020-j140	13	000-j410
5	006-j110	14	000-j380
6	004-j905	15	000-j355
7	002-j771	16	000-j333
8	001-j672		

Fig. 3. (a) The waveguide mixer used in the example, and (b) its equivalent circuit. The embedding impedance Z_e seen by the diode is tabulated as a function of harmonic number n. Guide impedance Z_g is given by (19). Parameter values are: $f_{LO} = 15$ GHz, $i_0 = 5$ nA, $\alpha = 40$ V^{-1}, $V_{bias} = 0$, $R_{dc} = 1.0$ Ω, $C = 0.2$ pF, $L = 0.72$ nH, $R_s = 5$ Ω, $D = 0.377$ in, and the waveguide is 0.070 in high × 0.662 in wide.

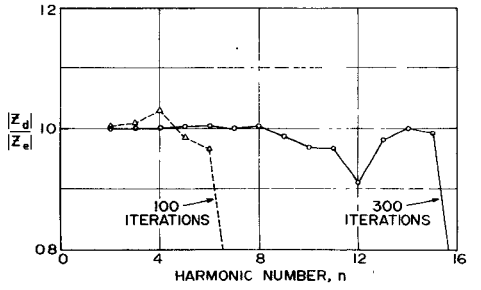

Fig. 4. Convergence parameter $|Z_d(nf_{LO})| / |Z_e(nf_{LO})|$ as a function of harmonic number n after 100 iterations (dashed curve) and 300 iterations (solid curve). For 500 iterations (not shown) all harmonics except the 16th were within 0.5 percent of unity.

Diode Capacitance and Series Resistance

In explaining the method of solution of the mixer problem it was convenient to assume a simple diode with no parasitic elements, as described by (1). We now apply the method to two more realistic diode models. The first, in which the diode capacitance C and series resistance R_s are both constant, requires no modification of the method. The elements C and R_s are simply considered as part of the embedding network and the problem is solved as before.

For the second diode model the capacitance and series resistance are functions of the diode terminal voltage. In this case the simple circuit of Fig. 2(a) is modified to include $C(v_d)$ and $R_s(v_d)$, and numerical integration of the circuit equations is necessary in order to determine the steady-state solutions for $v_d(t)$ and $i_d(t)$ each time Step 3 of the cycle is performed. The right-propagating wave $e_R(L,t)$ now produces an initial transient response at the diode which must be allowed to die away before the steady-state values of v_d, i_d, and $e_L(L,t)$ are calculated. This situation is the same as occurs at the embedding network when a new wave $e_L(0,t)$ arrives at it.

III. EXAMPLE

To test the method a computer program was written which determines the diode waveforms i_d and v_d in the waveguide mixer of Fig. 3. The diode is mounted across the middle of a reduced-height waveguide, and connected through a coaxial RF choke to the bias and IF circuits. To one side of the diode there is a waveguide short circuit at a distance D, and on the other side the diode sees the guide impedance

$$Z_g(f) = 2\left(\frac{\mu}{\epsilon}\right)^{1/2}\frac{b}{a}\frac{1}{[1-(f_c/f)^2]^{1/2}}. \tag{19}$$

The impedance of the embedding network, including the RF choke and the shorted waveguide section, is calculated at each LO harmonic. This characterization of the mixer is not an accurate representation at the harmonics of the LO frequency [5], [6], but it

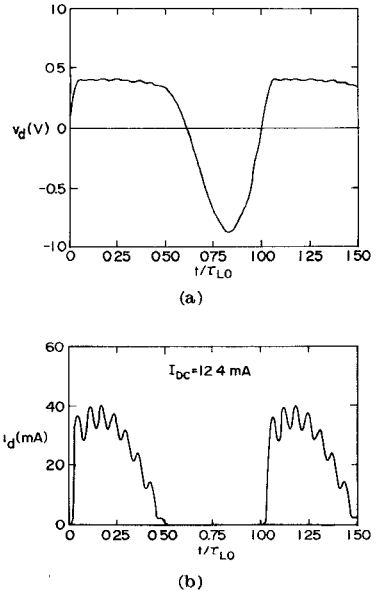

Fig. 5. (a) Diode voltage. (b) Diode current for the mixer shown in Fig. 3, after 500 iterations, considering 16 harmonics of the LO frequency. Time t is normalized to the LO period τ_{LO}.

provides a useful approximation for the purposes of this example. The embedding impedance Z_e seen by the diode at the LO frequency and its harmonics is tabulated in Fig. 3.

Fig. 4 shows the convergence parameter $|Z_d(jn\omega_{LO})|/|Z_e(jn\omega_{LO})|$ as a function of harmonic number n, when 16 harmonics are considered. For 300 iterations, convergence is reasonably complete up to the 11th harmonic. For 500 iterations $|Z_d|$ is within 0.5 percent of $|Z_e|$ up to the 15th harmonic.

The diode current and voltage waveforms are shown in Fig. 5. The computation time per cycle of iteration, when 16 harmonics are considered, is 3 ms on an IBM 360/95, and 2 s on an IBM 360/50.

REFERENCES

[1] H. C. Torrey and C. A. Whitmer, *Crystal Rectifiers* (M. I. T. Radiation Lab. Ser., vol. 15). New York: McGraw-Hill, 1948.

[2] D. A. Fleri and L. D. Cohen, "Nonlinear analysis of the Schottky-barrier mixer diode," *IEEE Trans. Microwave Theory Tech.*, vol. MTT-21, pp. 39–43, Jan. 1973.

[3] S. Egami, "Nonlinear, linear analysis and computer-aided design of resistive mixers," *IEEE Trans. Microwave Theory Tech. (Special Issue on Computer-Oriented Microwave Practices)*, vol. MTT-22, pp. 270–275, Mar. 1974.

[4] W. K. Gwarek, "Nonlinear analysis of microwave mixers," M. S. thesis, Mass. Inst. Technol., Cambridge, Sept. 1974.

[5] A. R. Kerr, "Low-noise room-temperature and cryogenic mixers for 80–120 GHz," this issue, pp. 781–787.

[6] R. L. Eisenhart and P. J. Khan, "Theoretical and experimental analysis of a waveguide mounting structure," *IEEE Trans. Microwave Theory Tech.*, vol. MTT-19, pp. 706–719, Aug. 1971.

Wide-Band Characteristics of a Coaxial-Cavity Solid-State Device Mount

PHILIP H. ALEXANDER, MEMBER, IEEE, AND PETER J. KHAN, MEMBER, IEEE

***Abstract*—An experimental comparison is made between two theoretical approaches to evaluation of the driving-point impedance at the terminals of a gap in the center conductor of a coaxial cavity. The study shows that for wide-band characterization, radial-wave modal-field analysis provides greater accuracy than the conventional transmission-line approach.**

I. INTRODUCTION

This short paper reports a comparison between two methods for the analysis of a coaxial cavity over a wide frequency range. The cavity, shown in Fig. 1, is assumed to be formed of perfectly conducting material, and contains a gap in the center conductor, within which a solid-state device may be located. The purpose of the study was to determine the driving-point impedance (i.e., the reactance of the lossless structure) viewed from the gap terminals, for a wide range of frequencies and cavity dimensions.

Attention has previously been confined to the lowest order resonance of the cavity, using Green's function [1] and radial line analyses [2], [3], in addition to conventional TEM-mode transmission-line theory. Our interest in wide-band characterization arises from the need for knowledge of harmonic-frequency impedance values in the design of solid-state oscillators [4], [5].

Manuscript received May 13, 1974; revised April 14, 1975. This work was supported by NSF Grant GK-32370.

P. H. Alexander was with the Cooley Electronics Laboratory, Department of Electrical and Computer Engineering, University of Michigan, Ann Arbor, Mich. 48105, on leave from the Department of Electrical Engineering, University of Windsor, Windsor, Ont., Canada. He is now with the Department of Electrical Engineering, University of Windsor, Windsor, Ont., Canada.

P. J. Khan is with the Cooley Electronics Laboratory, Department of Electrical and Computer Engineering, University of Michigan, Ann Arbor, Mich. 48105.

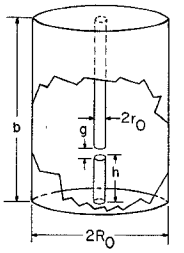

Fig. 1. Lossless coaxial cavity for use as a solid-state device mount.

II. THEORETICAL ANALYSIS

Two approaches to determination of the impedance viewed from the center-conductor gap are described briefly here.

A. Transmission-Line Analysis

This analysis yields the circuit shown in Fig. 2. The inductance L accounts for magnetic energy storage in the annular region of length g, external to the gap. The capacitances C_1' and C_2 represent the gap discontinuity, determined from the approach of Green [6] and Dawirs [7]. C_1' represents the series gap capacitance of these authors, modified by subtraction of a parallel-plate capacitance C_0, since we are interested in the impedance which loads a packaged device mounted in the gap; this distinction has also been made by Getsinger [8]. Using Fig. 2, the susceptance $B_R = -1/X_R$ is given by

$$B_R = \omega C_1' - [\omega L + Z_0(T_1 \tan \beta l_1 + T_2 \tan \beta l_2)]^{-1} \qquad (1)$$

where

$$T_i = (1 - \omega C_2 Z_0 \tan \beta l_i)^{-1}, \qquad \text{for} \quad i = 1,2.$$

B. Radial-Wave Analysis

The input reactance is calculated by establishing two sets of radial waves, outward bound and inward traveling, and imposing perfect-conductor boundary conditions at $r = R_0$. Using the concept of complex Poynting vector power, the radiation impedance at the gap terminals is determined by an approach similar to that of Eisenhart and Khan [9]; this impedance reduces to a reactance jX_R for the lossless structure considered here. Summing over all possible modes, we obtain

$$B_R = \sum_{n=0}^{\infty} \frac{(K_{gn})^2}{Z_n}$$

where

$$Z_n = j\left[\frac{(1+\delta_{n0})b\eta}{4\pi r_0}\frac{\beta_n}{k}\right]\left[\frac{J_0(\beta_n r_0)Y_0(\beta_n R_0) - J_0(\beta_n R_0)Y_0(\beta_n r_0)}{J_1(\beta_n r_0)Y_0(\beta_n R_0) - J_0(\beta_n R_0)Y_1(\beta_n r_0)}\right]$$

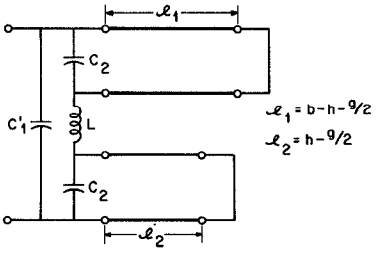

Fig. 2. Equivalent circuit of the driving-point reactance, using the transmission-line approach.